NANOSYSTEMS: PHYSICS, CHEMISTRY, MATHEMATICS, 2014, 5 (1), P. 117–122

INVESTIGATION OF STRUCTURE AND TRANSPORT PROPERTIES OF GRAPHENE GROWN BY LOW-PRESSURE NO FLOW CVD ON POLYCRYSTALLINE Ni FILMS

O. V. Kononenko[1*], V. N. Matveev[1], D. P. Field[2], D. V. Matveev[3], S. I. Bozhko[3], D. V. Roshchupkin[1], E. E. Vdovin[1]. A. N. Baranov[4]

[1]Institute of Microelectronics Technology and High Purity Materials, Russian Academy of Sciences, Chernogolovka, Russia
[2]School of Mechanical and Materials Engineering, Washington State University, Pullman, WA
[3]Institute of Solid State Physics, Russian Academy of Sciences, Chernogolovka, Russia
[4]Moscow State University, Moscow, Russia

*oleg@iptm.ru

PACS 68.65.Pq; 81.05.ue; 73.50.Jt

Graphene films were synthesized by the low-pressure no flow CVD on polycrystalline nickel catalyst films grown by the self-ion assisted deposition technique at different biases. Graphene films were transferred to a SiO_2/Si substrate using PMMA. The graphene grown on Ni films with bimodal grain size distribution and weaker (111) texture had higher thickness uniformity and a lower number of graphene layers. The graphene grown on Ni films with a monomodal grain size distribution and stronger (111) texture had lower thickness uniformity and a higher number of graphene layers. The transport properties of the graphene films were investigated with the aid of Hall measurements.

Keywords: Graphene, CVD Synthesis, Electronic properties.

1. Introduction

Among various carbon nanostructures, graphene as a single atom two-dimensional (2D) sp^2 hybrid carbon sheet shows unique properties for fundamental research [1–4] and promising applications in condensed-matter physics, electronics, and materials science. The interest in graphene-based structures has increased tremendously after the empirical discovery of graphene sheets in 2004 [5].

It is highly desirable to develop reliable synthesis techniques to fabricate graphene films. Recently we have developed a method to grow graphene films by low-pressure no flow CVD using thin Ni films deposited on SiO_2/Si substrates. As was shown earlier, the quality and uniformity of graphene films strongly depend on the structure of Ni films [6–9].

The graphene growth mechanism during CVD consists of several stages. The first is decomposition of a carbon containing precursor. The second is diffusion of carbon into bulk Ni, and the third is segregation and precipitation of carbon onto the Ni surface. If Ni films contain numerous defects, such as grain boundaries, triple junctions and dislocations which are good sinks for impurities, then carbon accumulates at these sites during the segregation stage leading to the formation of multilayer graphene [6–9].

As we showed in previous works [10, 11], the self-ion assisted deposition (SIAD) technique is a powerful method for control of microstructure of thin metal films. Due to the self-ion bombardment, high purity films are obtained during deposition.

2. Experimental

The Ni films were deposited by the self-ion assisted deposition technique on oxidized Si(100) substrates at 0 and -5 kV biases. High purity Ni (99.9999) was used as a source. The vacuum during deposition was about 10^{-6} torr. During deposition, the accelerating voltage was held at 0 or -5 kV. The thickness of the films was about 0.38 μm. After Ni deposition substrates were placed in a quartz tube reactor, which was pumped down to a pressure about 10^{-6} torr and then inserted into a preheated to 950 °C furnace. When the samples were heated to the reaction temperature, acetylene was admitted into the quartz tube up to a pressure of 0.4 torr for 5 s and then pumped out and the quartz tube reactor was extracted from the furnace.

X-ray diffraction (XRD) spectra were measured before and after graphene growth with a Bruker D8 DISCOVER diffractometer.

Crystallographic texture of the tested films was performed by orientation imaging microscopy [12, 13] using a field emission scanning electron microscope (FESEM). Electron backscatter diffraction (EBSD) technology was used for obtaining diffraction patterns over a regular array for each film examined. Inherent in the orientation imaging technique is complete crystallographic information that describes the spatial arrangement of texture and microtexture.

Transfer of the resulting graphene was done with the aid of poly(methyl methacrylate) (PMMA) that was spincoated on the surface of the graphene film to serve as a support. The PMMA/graphene layer was detached from the substrate by wet-etching of the Ni film with a 1 wt% aqueous solution of hydrochloric acid and then manually laid on the target substrate (SiO_2/Si). The PMMA was finally removed by exposure to acetone in vapor and then liquid form.

Raman spectra and mapping images of graphene films were measured with a Renishaw Raman microscope using a 633 nm excitation wavelength.

Hall measurements were performed to investigate transport properties of graphene films. Hall bar structures were fabricated using standard photo lithography and oxygen plasma etching.

3. Results and discussion

XRD spectra were collected from as-deposited Ni films and from Ni films after graphene synthesis (Fig. 1). The XRD spectra of as-deposited films showed strong Ni (111) peaks and weak Ni (200) peaks. Intensity of Ni (111) peak for the -5 kV film was stronger than that for the 0 kV film. Intensities of the Ni (111) and Ni (200) peaks increased in both films after graphene growth.

Figure 2 contains a representative orientation image of 0 and -5 kV Ni films after graphene synthesis. We observed that the Ni films deposited at -5 kV bias were strongly (111) textured. The average grain size was about 1 μm. Ni films deposited at 0 kV bias had (111) oriented grains and a noticeable fraction of (100) oriented grains. A bimodal grain size distribution was observed in the films. In a matrix of rather small grains (about 1.5 μm), a few larger grains (4–6 μm) were found.

Figure 3 shows back scattered electron images of the graphene films grown on Ni films deposited at 0 and -5 kV biases. Darker contrast corresponds to a thicker graphene films. It is seen that graphene film grown on the -5 kV Ni substrate consists of a larger number of layers.

In Raman spectroscopy graphene is typically characterized by a D-peak near 1300 – 1350 cm^{-1}, a G-peak near 1580 cm^{-1} and a 2D-peak near 2600 – 2700 cm^{-1} [14]. The relative intensities and the widths of the G and 2D peaks give us possibilities to judge about the number of layers in graphene films. Raman spectra were collected from graphene films grown on 0 and -5 kV biased Ni films and transferred to SiO_2/Si(100) substrates. The sharp peaks are

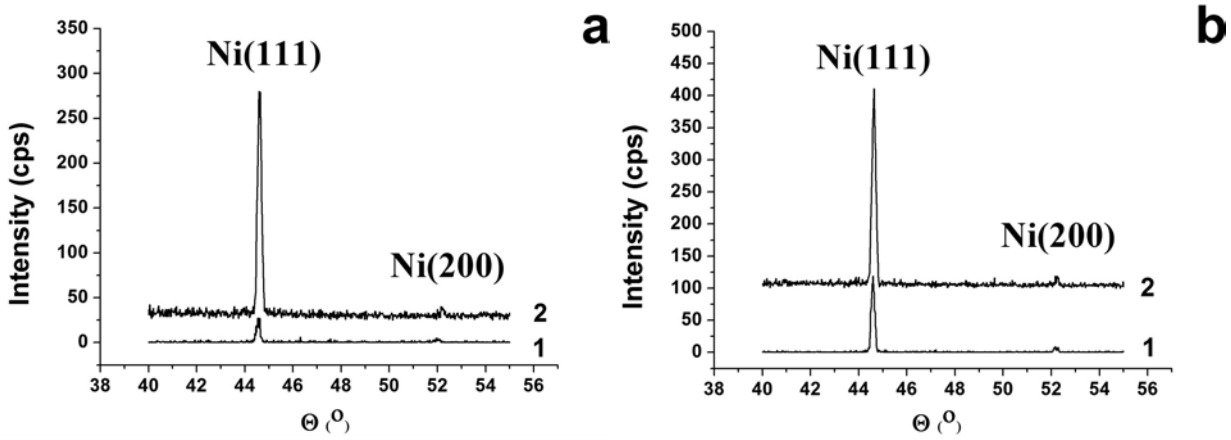

FIG. 1. a) XRD spectra collected from an as-deposited Ni film and b) from Ni films after graphene synthesis. Curves (1) correspond to films deposited at 0 kV bias and curves (2) correspond to films deposited at -5 kV bias

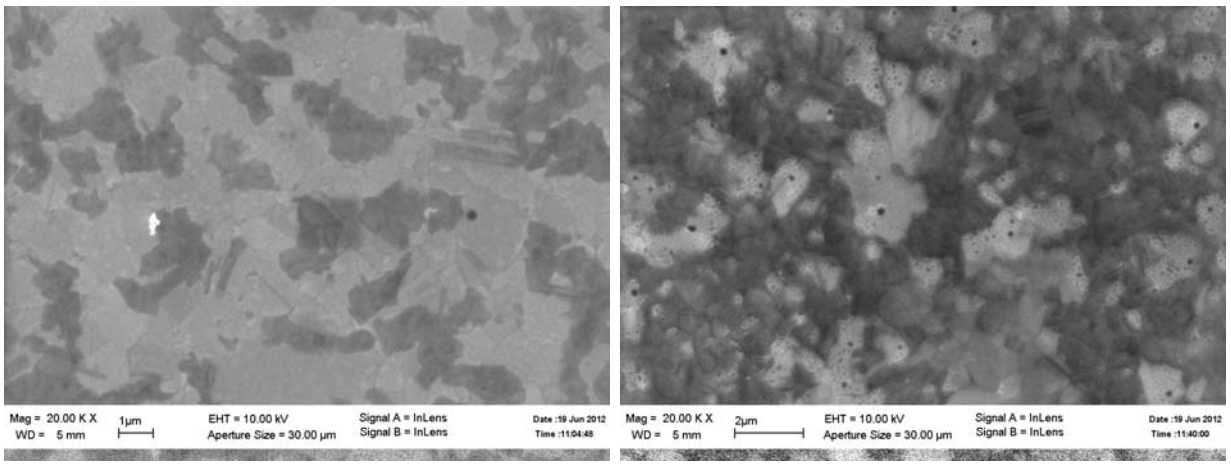

FIG. 2. Orientation images of the Ni films deposited at 0 (a) and -5 kV (b) bias obtained after graphene synthesis

indicative of the crystallinity of the films and the plot shows several distinct peaks, one at about 1582 – 1588 cm^{-1} (G peak) and the other at about 2650 – 2670 cm^{-1} (2D peak). The peak at around 1582 cm^{-1} is attributed to sp^2 phonon vibrations. The 2D peak is used to confirm the presence of graphene and it originates from a double resonance process that links phonons to the electronic band structure. A peak occurring at about 1320 – 1350 cm^{-1} (D band) indicates phonon scattering at defect sites and impurities. Spectra collected from graphene films, for the most part, show single Lorentzian lineshape and narrow linewidth.

Figure 4 contains a representative Raman spectra of transferred graphene films grown on 0 and -5 kV Ni films. The spectrum from graphene grown on the 0 kV Ni film (Fig. 4a) presents typical features for monolayer graphene: the I_{2D}/I_G intensity ratio is $\sim$1.85, and the full width at half-maximum (FWHM) of the 2D band is $\sim$65 cm^{-1}. Small D and D′ peaks (near 1620 cm^{-1}) indicates that some defects such as grain boundaries, vacancies and impurities are contained in the graphene film. The spectrum corresponding to graphene grown on the -5 kV Ni film (Fig. 4b) has a noticeable upshift of $\sim$15 cm^{-1} in the 2D band, as well as a broadening of the 2D band line width ($\sim$30 cm^{-1}) that can be fit with four or more Lorentzian peaks. The I_{2D}/I_G intensity ratio is $\sim$0.65, and the FWHM of the 2D band is $\sim$95 cm^{-1}. It

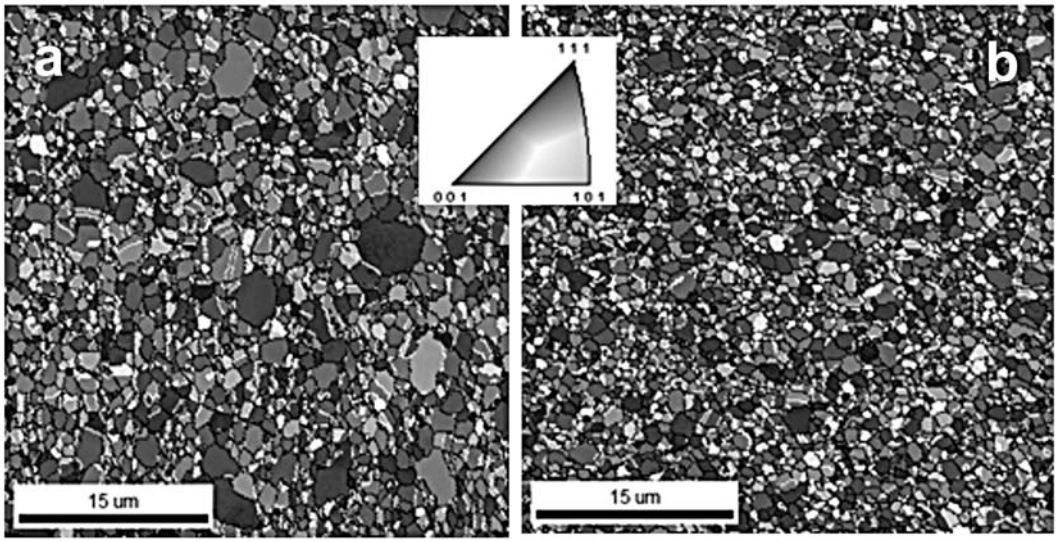

FIG. 3. Back scattered electron images obtained from Ni films deposited at 0 (a) and -5 kV (b) bias after graphene synthesis

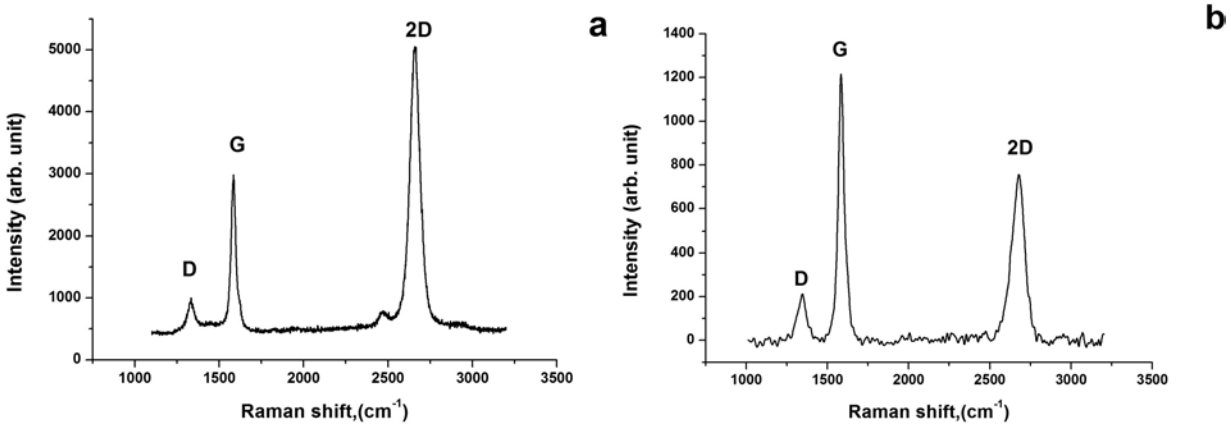

FIG. 4. Raman spectra collected from graphene films grown on 0 (a) and -5 kV (b) biased Ni films and transferred to SiO_2/Si(100) substrates

is known that the 2D peak position exhibits an upshift with an increased number of graphene layers , and the fitting of the 2D peak with two or more Lorentzian peaks is a signature of multilayer graphene. The I_{2D}/I_G intensity ratio is smaller than one, which also is characteristic of multilayer graphene [15–17].

Raman spectra were collected from both types of graphene films over 2000 μm^2 area. The I_{2D}/I_G values were then extracted from the spectra. Fig. 5 show the I_{2D}/I_G contour maps for graphene grown on 0 and -5 kV-biased Ni films (a and b, respectively), on an oxidized silicon substrate. Nearly 74% of Raman spectra collected from the graphene grown on 0 kV bias Ni films shows the hallmark of monolayer/bilayer graphene and about 25% indicates multi-layer graphene. Graphene films grown on -5 kV bias Ni films demonstrated only about 33% of monolayer/bilayer character, while 67% was multi-layer graphene. Thus, the graphene grown on Ni films with a bimodal grain size distribution and weaker (111) texture had higher thickness uniformity and lower number of graphene layers. Conversely, the graphene grown on Ni films with a monomodal grain size distribution and stronger (111) texture had lower thickness uniformity and a higher number of graphene layers.

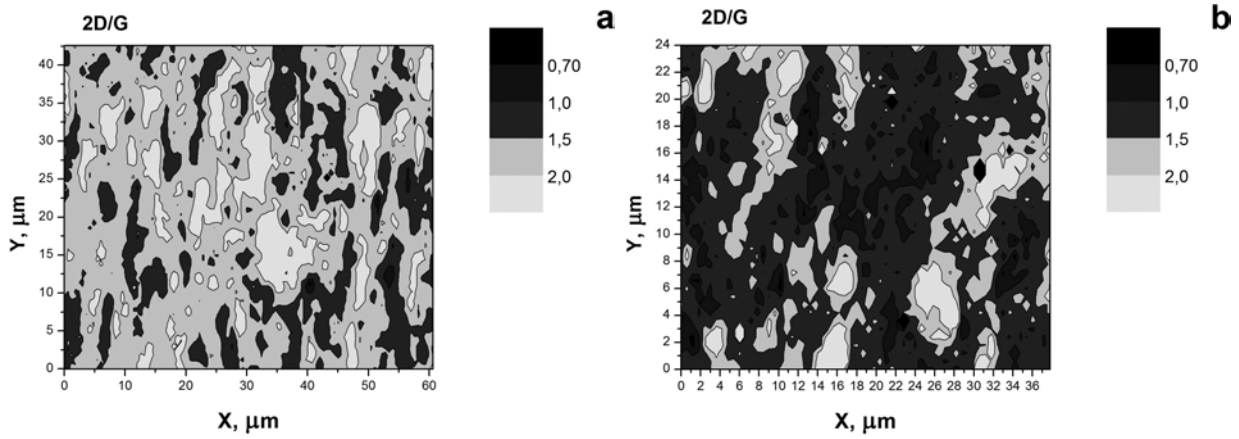

FIG. 5. I_{2D}/I_G contour maps of graphene grown on 0 (a) and -5 kV (b) biased Ni films and transferred to SiO_2/Si (100) substrates

The transport properties of Ni-supported graphene films deposited at 0 kV bias were investigated. The most direct and precise method to measure the mobility is the Hall measurement. The sheet resistance (Rs) of the graphene was measured at 900 Ohm/square from the four probe method. Subsequently, the Hall mobility is derived from:

$$\mu = \partial Rxy/\partial B/Rs, \tag{1}$$

where B is the magnetic field perpendicular to the Hall bar plane. The measurement was taken at 4.2 K and the Hall mobility was about 1200 $cm^2/V{\cdot}s$. Thus, the film had p-type conductivity. The carrier density was about $10^{13}/cm^2$, determined from:

$$n_{Hall} = 1/eR_{Hall}. \tag{2}$$

The relatively lower mobility of the graphene is attributed to the nonuniformity of the film quality and the poor adhesion with substrates, damages of the graphene during transfer to the target substrate, and the residual resist and impurities on the surface of the graphene.

4. Conclusion

Graphene films were synthesized by the low-pressure no flow CVD on polycrystalline nickel films. Ni films were deposited by the self-ion assisted deposition technique at 0 and -5 kV biases. 0 kV Ni films possessed bimodal grain size distribution and weaker (111) texture. The graphene grown on that films with a bi-modal grain size had higher thickness uniformity and predominately consisted of a mono- or bilayer film. Ni films deposited at -5 kV bias had smaller grain size and stronger (111) texture. The graphene grown on these films had lower thickness uniformity and a higher number of graphene layers.

References

[1] Novoselov K.S., Geim A.K., et al. Two-dimensional gas of massless Dirac fermions in graphene. *Nature*, **438**, P. 197–200 (2005).

[2] Katsnelson M.I., Novoselov K.S. Graphene: New bridge between condensed matter physics and quantum electrodynamics. *Solid State Commun.*, **143**, P. 3–13 (2007).

[3] Meyer J.C., Geim A.K., et al. The structure of suspended graphene sheets. *Nature*, **446**, P. 60–63 (2007).

[4] Schedin F., Geim A.K., et al. Detection of individual gas molecules adsorbed on graphene. *Nature Mater.*, **6**, P. 652–655 (2007).

[5] Novoselov K. S., Geim A. K., et al. Electric Field Effect in Atomically Thin Carbon Films. *Science*, **306**, P. 666–669 (2004).
[6] Zhang Y., Gomez L., et al. Comparison of Graphene Growth on Single-Crystalline and Polycrystalline Ni by Chemical Vapor Deposition. *J. Phys. Chem. Lett.*, **1**, P. 3101–3107 (2010).
[7] Thiele S., Reina A., et al. Engineering polycrystalline Ni films to improve thickness uniformity of the chemical-vapor-deposition-grown graphene films. *Nanotechnology*, **21**, P. 015601 (2010).
[8] Liu N., Fu L., et al. Universal Segregation Growth Approach to Wafer-Size Graphene from Non-Noble Metals. *Nano Lett.*, **11**, P. 297–303 (2011).
[9] Reina A., Thiele S., et al. Growth of large-area single- and Bi-layer graphene by controlled carbon precipitation on polycrystalline Ni surfaces. *J. Nano Res.*, **2**, P. 509–516 (2009).
[10] Kononenko O.V., Matveev V.N., et al. The effect of self-ion bombardment on the properties of thin metal films. *Vacuum*, **46**, P. 685–690 (1995).
[11] Field D.P., Kononenko O.V., Matveev V.N. The microstructure of Cu films deposited by the self-ion assisted technique. *J. Electron. Mater.*, **31**, P. 40–44 (2002).
[12] Adams B.L., Wright S.I., Kunze K. Orientation imaging: The emergence of a new microscopy. *Metall. Trans.*, **24A**, P. 819–831 (1993).
[13] Krieger-Lassen N.C., Conradsen K., Juul-Jensen D. Image processing procedures for analysis of electron back scattering patterns. *Scanning Microscopy*, **6**, P. 115–121 (1992).
[14] Ferrari A.C. Raman spectroscopy of graphene and graphite: Disorder, electron-phonon coupling, doping and nonadiabatic effects. *Solid State Commun.*, **143**, P. 47–57 (2007).
[15] Gupta A., Chen G., et al. Raman Scattering from High-Frequency Phonons in Supported N-Graphene Layer Films. *Nano Lett.*, **6**, P. 2667–2673 (2006).
[16] Ferrari A.C., MeyerJ.C., et al. Raman Spectrum of Graphene and Graphene Layers. *Phys. Rev. Lett.*, **97**, P. 187401 (2006).
[17] Cancado L.G., Reina A., Kong J., Dresselhaus M.S. Geometrical Approach for the Study of G' Band in the Raman Spectrum of Monolayer Graphene, Bilayer Graphene, and Bulk Graphite. *Phys. Rev. B*, **77**, P. 245408 (2008).